Electronic Supplementary Material (ESI) for Journal of Materials Chemistry C.
This journal is © The Royal Society of Chemistry 2024

Modulation Acceptor of Covalent Organic Frameworks: The Optimization of Intramolecular and Interfacial Charge Transfer Processes

Ziang Song[a], Yujun Xie[a], Xiaojuan Song[a], Jianing Tang[a], Jinfeng Wang*[a], Ben Zhong Tang*[a, c] and Zhen Li*[a, b, d]

Affiliations:

[a] Institute of Molecular Aggregation Science, Tianjin University, Tianjin 300072, China

[b] Joint School of National University of Singapore and Tianjin University, International Campus of Tianjin University Binhai New City, Fuzhou, Fujian, 350207, China

[c] School of Science and Engineering, Shenzhen Institute of Aggregate Science and Technology, The Chinese University of Hong Kong, Shenzhen, Guangdong, 518172, China.

[d] Hubei Key Lab on Organic and Polymeric Opto-Electronic Materials, Department of Chemistry, Wuhan University, Wuhan, Hubei, 430072, China

Emails: jinfeng.wang@tju.edu.cn, tangbenz@cuhk.edu.cn, lizhen@whu.edu.cn.

Table of Contents

Section I. Materials and Characterization

1. Materials

All reagents and solvents were purchased from commercial sources and used directly without further purification.

2. General characterization

The ^{1}H and ^{13}C NMR were obtained with 400 MHz Bruker Ascend 400 MHz NMR spectrometer. High resolution mass spectrometry (HRMS) data were collected on RDa time of flight Mass Detector (Waters, USA) coupled with ACQUITY UPLC (Waters, USA). The Solid-state nuclear magnetic resonance (^{13}C CP/MAS NMR) spectra were obtained with a JEOL JNM ECZ600R. The Powder X-ray diffraction (PXRD) patterns were recorded on a Rigaku MiniFlex600 diffractometer equipped with Cu/Kα radiation (λ = 1.5418 Å) under a scan rate of 10 degree/min. The Fourier transform infrared spectroscopy (FT-IR) spectra were performed on ThermoFisher Scientific Nicolet IN10 in the frequency range of 674-4000 cm^{-1}, using ATM mode. The X-ray photoelectron spectroscopy (XPS) spectra was measured by using ThermoFisher Scientific EscaLab 250 xi. Scanning electron microscopy (SEM) images was performed on HITACHI SU8010 with an accelerating voltage of 12.0 kV. Transmission electron microscopy (TEM) images were recorded on a TecnaiG2F20 electron microscope (200 kV) equipped with slow scan CCD using cold cathode field emission as the gun. The nitrogen adsorption-desorption isotherm measurements were carried out using a Micromeritics ASAP2460 with extra-high pure gases. Before the gas adsorption measurements, the samples (80 mg) were activated and degassed at 120 °C for 12 h. The resulting samples were then used for gas adsorption measurements from 0 to 1 atm at 77 K. The Brunauer-Emmett Teller (BET) surface area and total pore volume were calculated from the N_2 sorption isotherms, and the Density Functional Theory (DFT) pore size distribution was calculated based on the N_2 sorption isotherm by using an equilibrium model and assuming a cylindrical pore geometry. Thermogravimetric analysis (TGA) was evaluated by NETZSCH TG 209F3 analyzer over the temperature range from 40 to 800 °C in N_2 with a heating rate of 10°C/min. Solid-state UV-Vis DRS spectra of the COF powders were measured on a Shimadzu UV-3600 spectrometer. Photoluminescence (PL) spectra and time-correlated single photon counting measurements were collected on Edinburgh Instruments FLS1000 fluorescence spectrophotometer.

3. Photocatalytic measurements

Photocatalytic hydrogen evolution measurements were carried out on a closed gas system equipped with a top-irradiation-type vessel. Typically, 5 mg of COFs powder was ultrasonically dispersed in an aqueous solution (100 mL) containing ascorbic acid (0.1 M) as the sacrificial agent, and corresponding content of $H_2PtCl_6{\cdot}6H_2O$ as Pt precursor. The air in the system was removed completely by bubbling N_2 for 30 min before 300 W Xe lamp irradiation. The amount of H_2 evolved was determined by gas chromatography (Shimadzu GC-2014C, thermal conductivity detector (TCD), N_2 carrier).

4. The apparent quantum efficiency (AQE) measurements

The AQE for hydrogen evolution was measured under the illumination of a 300 W Xe lamp equipped with different band-pass filters (365 nm, 420 nm and 500 nm). The light densities (mW·cm^{-2}) were measured based on previous reports[1,2] and the densities of each monochromatic wavelength are 3.88, 8.13, 16.51 mW/cm^2, respectively. The irradiation area was a circular area with a radius of 3 cm. The calculation formula is as follows:

$$\eta_{AQE} = \frac{Number\ of\ reacted\ electrons}{Number\ of\ incident\ electrons} \times 100\% = \frac{2 \times M \times N_A}{\frac{S \times P \times t}{h \times \frac{c}{\lambda}}} \times 100\% = \frac{2}{} \times 100\%$$

Where, M is the amount of H_2 molecules (mol), N_A is Avogadro constant (6.022 ×10^{23} mol^{-1}), h is the Planck constant (6.626 × 10^{-34} J·s), c is the speed of light (3 ×10^8 m·s^{-1}), S is the irradiation area (cm^2), P is the density of irradiation light (W·cm^{-2}), t is the photoreaction time (s), λ is the wavelength of the monochromatic light (nm).

5. Photocurrents and photoelectrochemical measurements

All of the photoelectrochemical measurements were obtained on an electrochemical workstation (CHI660E, CH Instrument Corp, Shanghai) using a standard three-electrode cell at room temperature under irradiation of a 300 W Xe lamp (Perfect Light PLSSXE 300+/UV, λ > 420 nm, 100 mW·cm^{-2}). The FTO glass (1×2 cm^2) coated with COFs (effective area of 1×1 cm^2) as the photoelectrode, Pt sheet electrode as the counter electrode, and an Ag/AgCl electrode as the reference electrode. The three electrodes were immersed in a quartz cell filled with Na_2SO_4 solution (0.2 M). The Na_2SO_4 electrolyte was purged with N_2 for 1 h before the measurements. For photocurrent intensity response experiments, the parameters are set as follows: initial voltage was 0.8 V, test time was 420 s, static time was 5 s, and the sensitivity was 10^{-6} A·V^{-1}. For electrochemical impedance spectroscopy measurements, the parameters are set as follows: initial voltage was open-circuit voltage, the highest frequency was 10000 Hz, the lowest frequency was 0.01 Hz, the amplitude was 0.005 V, and static time was 2 s. For Mott-Schottky measurements, the initial voltage was open-circuit voltage, the amplitude was 0.005 V, the static time was 2 s, and the frequency was 1000, 1500 and 2000 Hz. The applied potentials vs. Ag/AgCl ($E_{Ag/AgCl}$) were converted to RHE potentials (E_{RHE}) using the following equation:

$$E_{RHE} = E_{Ag/AgCl} + 0.0591pH + \varphi_{Ag/AgCl} \quad (\varphi_{Ag/AgCl} = 0.199\ V)$$

6. Method for DFT calculations

The optimized molecular structures, HOMO and LUMO energy level based on the segments of these COFs were carried out by Density functional theory (DFT) calculations, which were conducted by the

Gaussian 09 software at B3LYP/6-31G(d) level.[3]

Section II. Synthetic procedures

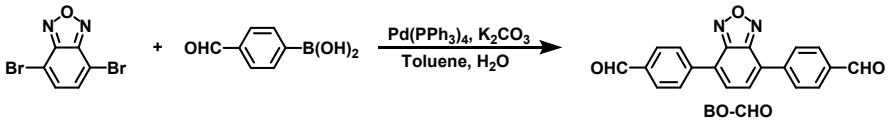

Scheme S1. The synthetic route of **BO-CHO**.

Synthesis of 4,4'-(benzo[c][1,2,5]oxadiazole-4,7-diyl)dibenzaldehyde (BO-CHO):
(4-formylphenyl)boronic acid (1.12 g, 7.5 mmol), 4,7-dibromobenzo[c][1,2,5]oxadiazole (0.83 g, 3.0 mmol) and $Pd(PPh_3)_4$ (0.17 g, 0.15 mmol) were added to a 100 mL Schlenk tube, which was degassed with nitrogen three times. Then the deoxygenated K_2CO_3 aqueous solution (2 M, 15 mL) and toluene (48 mL) were added to the Schlenk tube and refluxed for 12 h. After cooling to room temperature, the mixture was poured into the water and extracted with dichloromethane for three times. Then organic phase was dried by anhydrous sodium sulfate, then filtered, and the filtrate was collected. After evaporating the solvent, the crude product was purified by column chromatography (silica gel, petroleum ether: dichloromethane = 1:3) to afford a light yellow solid (0.49 g, yield 50%).^{1}H NMR (400 MHz, Chloroform-*d*) δ (TMS, ppm): 10.13 (s, 2H), 8.25 (d, *J* = 8.3 Hz, 4H), 8.08 (d, *J* = 8.4 Hz, 4H), 7.84 (s, 2H). ^{13}C NMR (101 MHz, Chloroform-*d*) δ (ppm): 191.71, 149.10, 140.65, 136.79, 130.43, 129.78, 129.19, 128.98. HRMS (ESI, m/z): $[M+H]^+$ calculated for $C_{20}H_{13}N_2O_3$: 329.0921, found 329.0941.

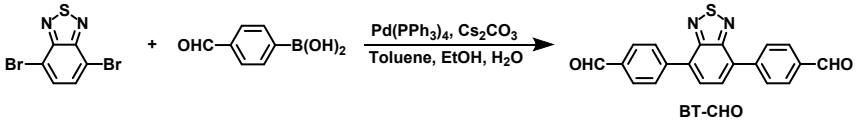

Scheme S2. The synthetic route of **BT-CHO**.

Synthesis of 4,4'-(benzo[c][1,2,5]thiadiazole-4,7-diyl)dibenzaldehyde (BT-CHO):
Compound **BT-CHO** was synthesized according to the previous literature.[4] (4-formylphenyl)boronic acid (1.12 g, 7.5 mmol), 4,7-dibromobenzo[c][1,2,5]thiadiazole (0.88 g, 3.0 mmol) and $Pd(PPh_3)_4$ (0.17 g, 0.15 mmol) were added to a 100 mL Schlenk tube, which was degassed with nitrogen three times. Then the deoxygenated Cs_2CO_3 aqueous solution (2 M, 7.5 mL), toluene (22.5 mL) and EtOH (15 mL) were added to the Schlenk tube and refluxed for 12 h. After cooling to room temperature, the mixture was poured into the water and extracted with dichloromethane for three times. The organic phase was dried by anhydrous sodium sulfate, then filtered, and the filtrate was collected. After evaporating the solvent, the crude product was purified by column chromatography (silica gel, petroleum ether: dichloromethane = 1:2) to afford a light yellow solid (0.73 g, yield 70%). ^{1}H NMR (400 MHz, Chloroform-*d*) δ (TMS, ppm): 10.13 (s, 2H), 8.18 (d, *J* = 8.2 Hz, 4H), 8.08 (d, *J* = 8.3 Hz, 4H), 7.92 (s, 2H). ^{13}C NMR (101 MHz, Chloroform-*d*) δ (ppm): 191.94, 153.92, 143.08, 136.22, 133.16, 130.14,

130.08, 128.83. HRMS (ESI, m/z): $[M+H]^+$ calculated for $C_{20}H_{13}N_2O_2S$: 345.0692, found 345.0684.

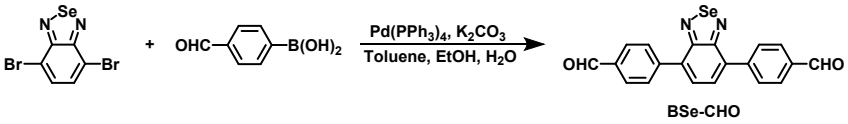

Scheme S3. The synthetic route of **BSe-CHO**.

Synthesis of 4,4'-(benzo[c][1,2,5]selenadiazole-4,7-diyl)dibenzaldehyde (BSe-CHO):

(4-formylphenyl)boronic acid (0.75 g, 5.0 mmol), 4,7-dibromobenzo[c][1,2,5]selenadiazole (0.68 g, 2.0 mmol) and $Pd(PPh_3)_4$ (0.12 g, 0.1 mmol) were added to a 250 mL Schlenk tube, which was degassed with nitrogen three times. Then the deoxygenated K_2CO_3 aqueous solution (2 M, 10 mL), toluene (48 mL) and EtOH (32 mL) were added to the Schlenk tube and refluxed for 12 h. After cooling to room temperature, the mixture was poured into the water and extracted with dichloromethane for three times. The organic phase was dried by anhydrous sodium sulfate, then filtered, and the filtrate was collected. After evaporating the solvent, the crude product was purified by column chromatography (silica gel, petroleum ether: dichloromethane = 1:2) to afford a gold yellow solid (0.61 g, yield 78%). ^{1}H NMR (400 MHz, Chloroform-*d*) δ (TMS, ppm): 10.13 (s, 2H), 8.11–8.04 (m, 8H), 7.75 (s, 2H). ^{13}C NMR (101 MHz, Chloroform-*d*) *δ* (ppm): 192.30, 159.64, 144.10, 136.44, 135.21, 130.66, 130.33, 129.46. HRMS (ESI, m/z): $[M+H]^+$ calculated for $C_{20}H_{13}N_2O_2Se$: 393.0137, found 393.0153.

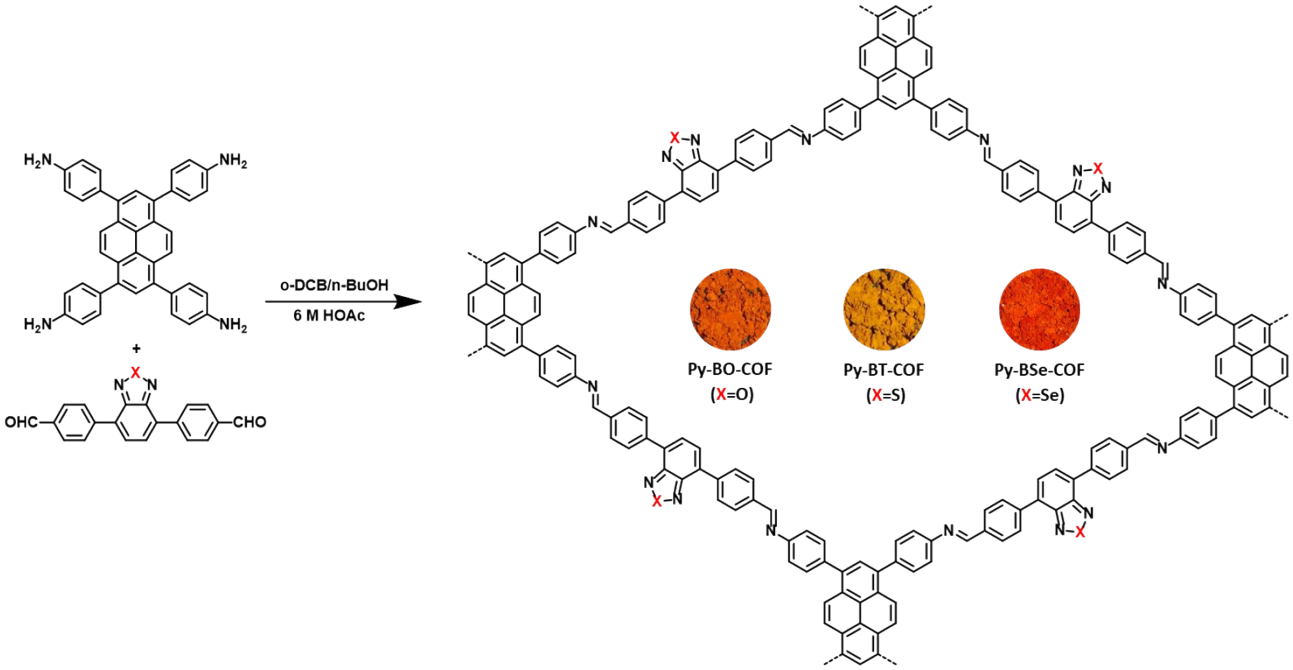

Scheme S4. The synthetic route of **Py-BO-COF**, **Py-BT-COF** and **Py-BSe-COF** .

Synthesis of Py-BO-COF:

BO-CHO (13.1 mg, 0.04 mmol), 4,4',4'',4'''-(pyrene-1,3,6,8-tetrayl)tetraaniline ($Py\text{-}NH_2$) (11.3 mg, 0.02 mmol), *o*-DCB (0.75 mL) and *n*-BuOH (0.25 mL) were added to a 20 mL Pyrex tube and sonicated for 5 min. Then acetic acid (6 M, 0.1 mL) was added and sonicated for another 5 min. The mixture was sealed under vacuum and then heated at 120 °C for 3 days. After cooling to room temperature,

the precipitate was collected by filtration, then washed with THF. Subsequently, the resulting solid was subjected to Soxhlet and extract with THF for 12 h. Finally, the collected sample was dried at 120 ^{o}C for 12 h to give an orange powder (21.4 mg, yield 93 %).

Synthesis of Py-BT-COF:

Py-BT-COF was synthesized based on the previous literature.[5] BT-CHO (13.8 mg, 0.04 mmol), Py-NH_2 (11.3 mg, 0.02 mmol), *o*-DCB (0.75 mL) and *n*-BuOH (0.25 mL) were added to a 20 mL Pyrex tube and sonicated for 5 min. Then of acetic acid (6 M, 0.1 mL) was added and sonicated for another 5 min. The mixture was sealed under vacuum and then heated at 120 °C for 3 days. After cooling to room temperature, the precipitate was collected by filtration and then washed with THF. Subsequently, the resulting solid was subjected to Soxhlet and extract with THF for 12 h. Finally, the collected sample was dried at 120 ^{o}C for 12 h to give a saffron yellow powder (21.1 mg, yield 89 %).

Synthesis of Py-BSe-COF:

BSe-CHO (15.7 mg, 0.04 mmol), Py-NH_2 (11.3 mg, 0.02 mmol), *o*-DCB (0.75 mL) and *n*-BuOH (0.25 mL) were added to a 20 mL Pyrex tube and sonicated for 5 min. Then acetic acid (6 M, 0.1 mL) was added and sonicated for another 5 min. The mixture was sealed under vacuum and then heated at 120 °C for 3 days. After cooling to room temperature, the precipitate was collected by filtration and then washed with THF. Subsequently, the resulting solid was subjected to Soxhlet and extract with THF for 12 h. Finally, the collected sample was dried at 120 ^{o}C for 12 h to give an orange powder (21.6 mg, yield 85 %).

Section III. Supplementary figures and tables

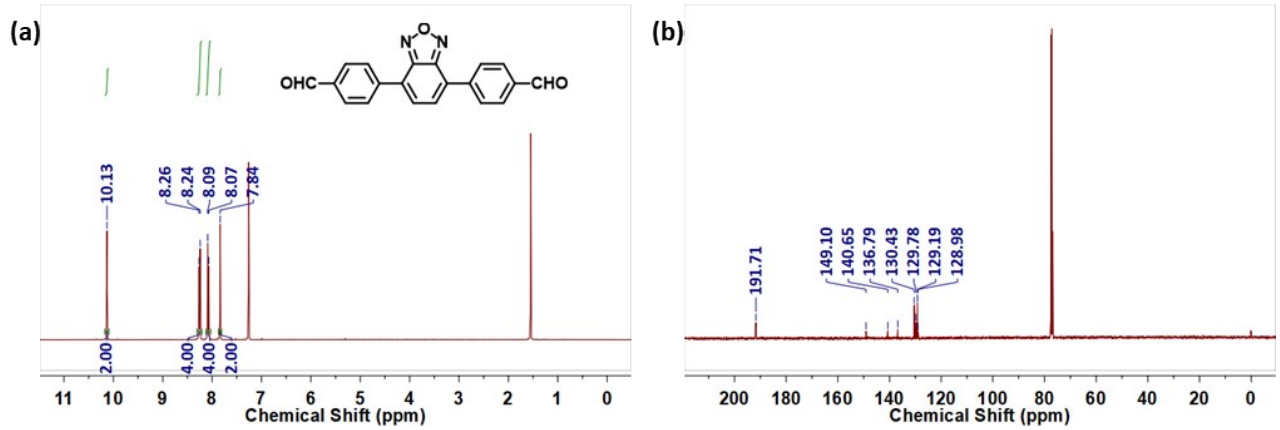

Fig. S1. (a) ^{1}H NMR and (b) ^{13}C NMR spectrum of **BO-CHO**.

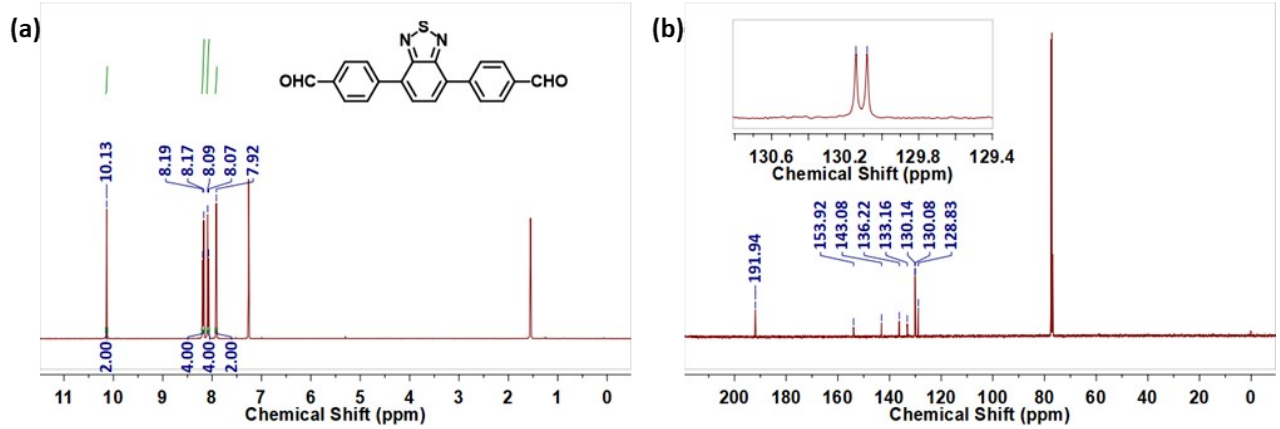

Fig. S2. (a) ^{1}H NMR and (b) ^{13}C NMR spectrum of **BT-CHO**.

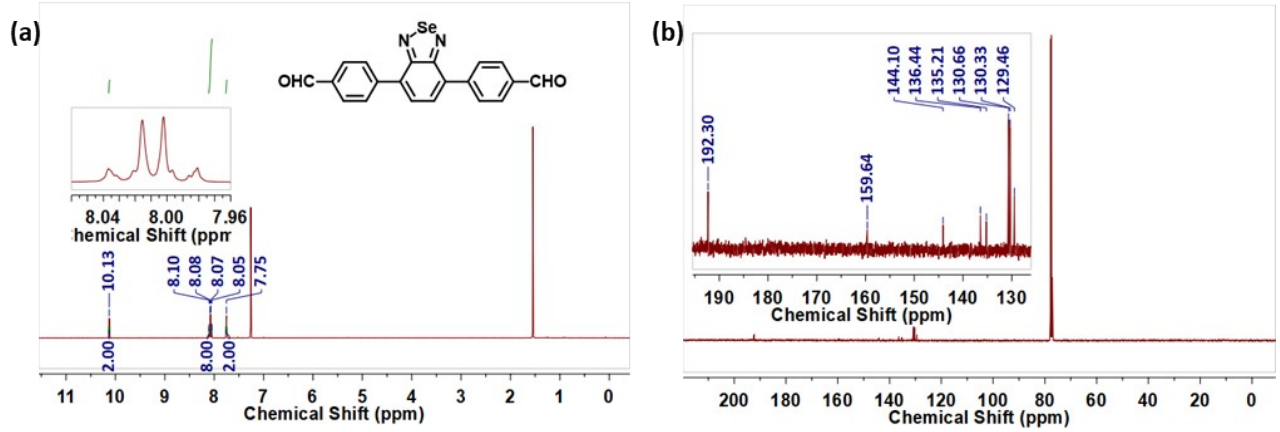

Fig. S3. (a) ^{1}H NMR and (b) ^{13}C NMR spectrum of **BSe-CHO**.

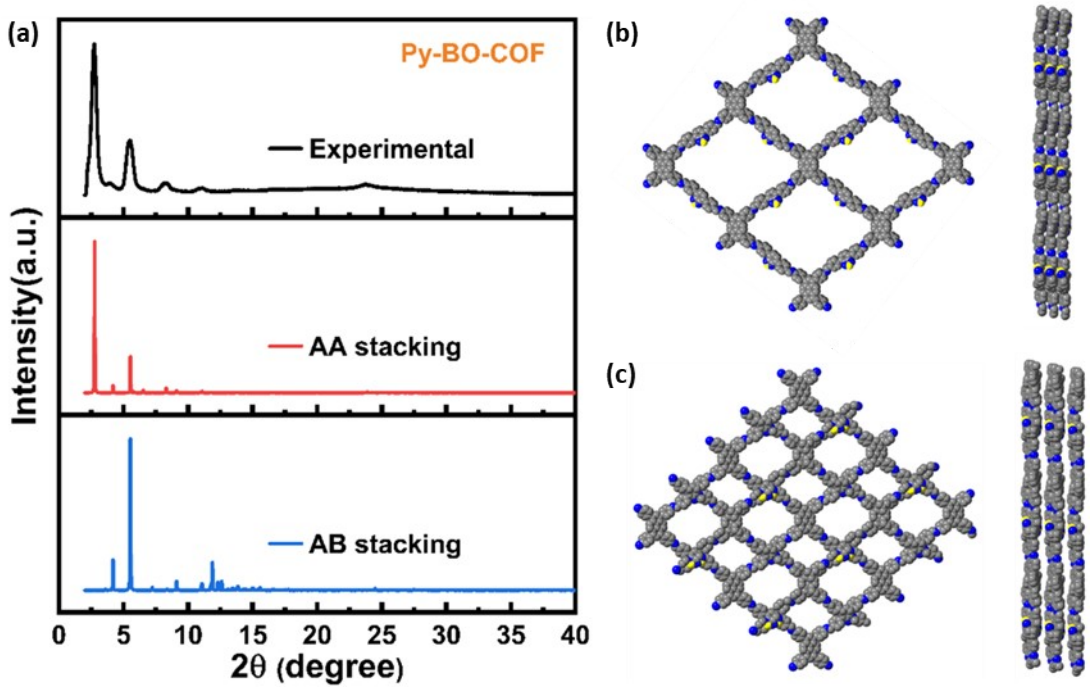

Fig. S4. (a) The experimental, simulated AA stacking, simulated AB stacking of Py-BO-COF; (b) top view and side view of simulated AA stacking; (c) top view and side view of simulated AB stacking.

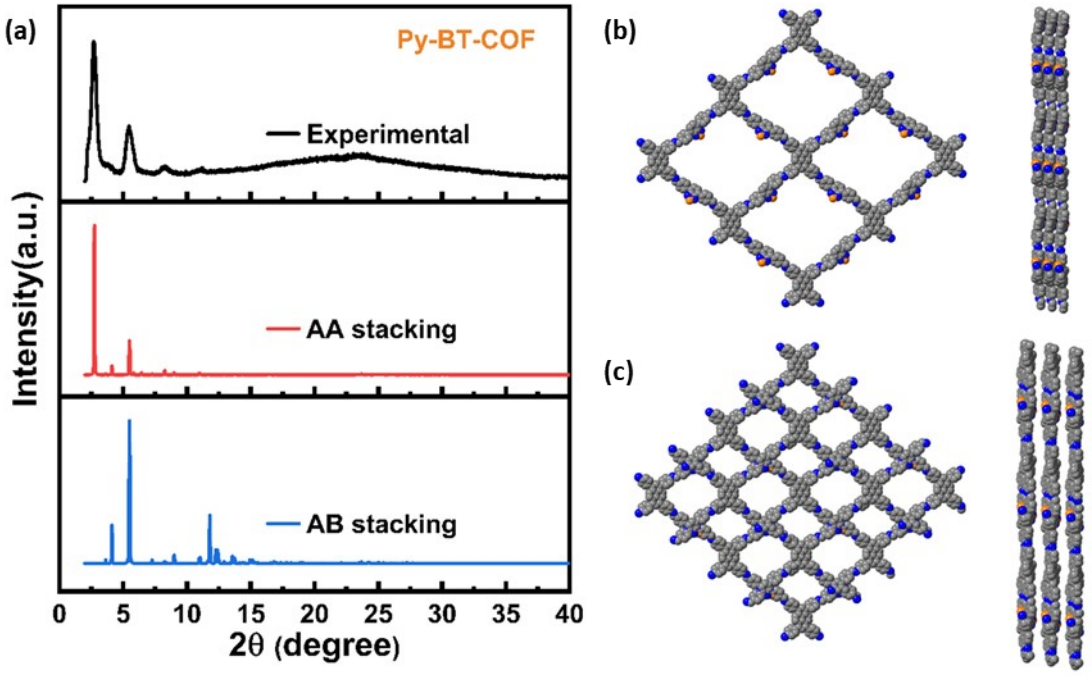

Fig. S5. (a) The experimental, simulated AA stacking, simulated AB stacking of Py-BT-COF; (b) top view and side view of simulated AA stacking; (c) top view and side view of simulated AB stacking.

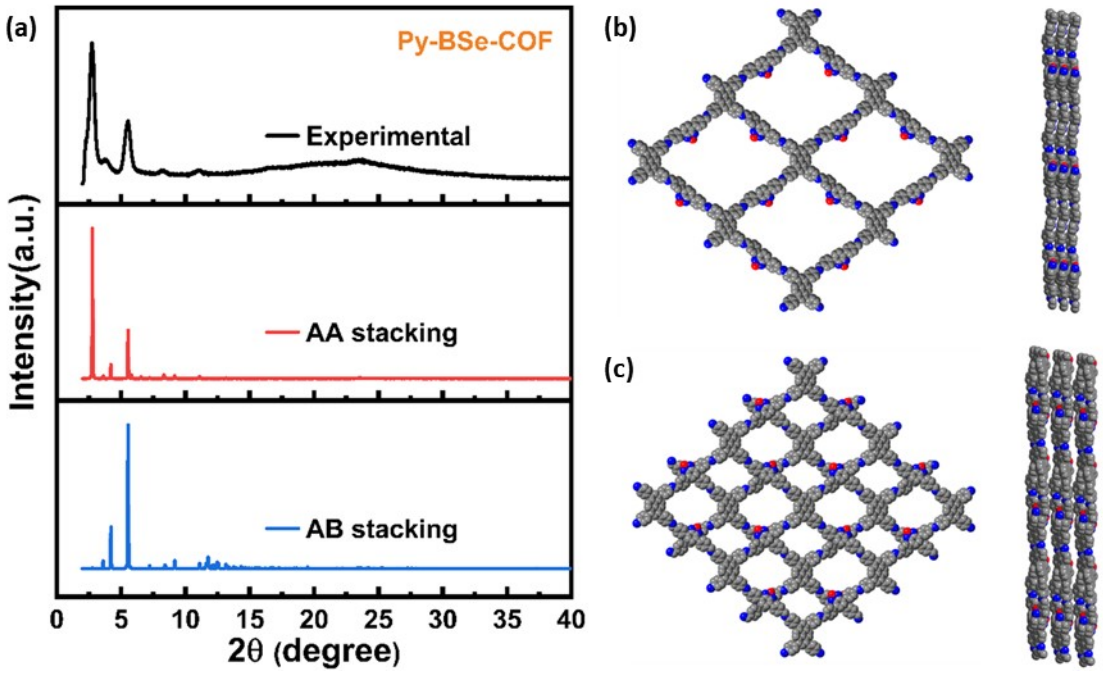

Fig. S6. (a) The experimental, simulated AA stacking, simulated AB stacking of Py-BSe-COF; (b) top view and side view of simulated AA stacking; (c) top view and side view of simulated AB stacking.

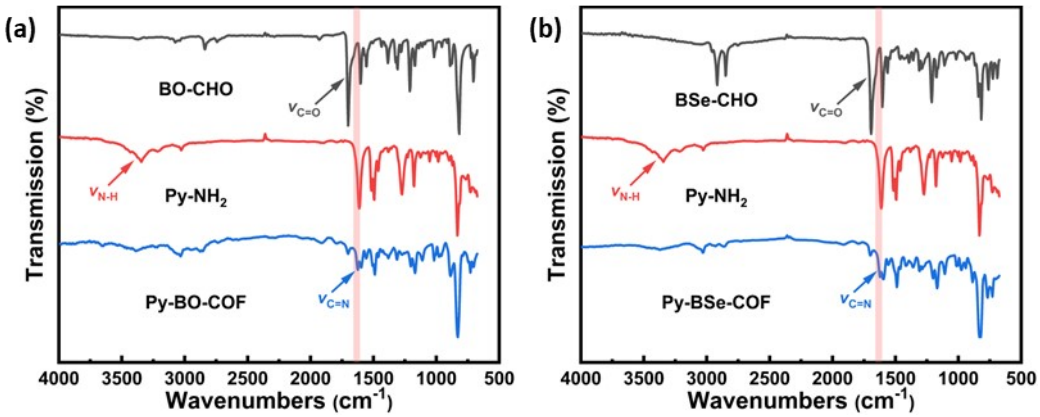

Fig. S7. FT-IR spectra of (a)BO-CHO, Py-NH_2 and Py-BO-COF, (b) BSe-CHO, Py-NH_2 and Py-BSe-COF.

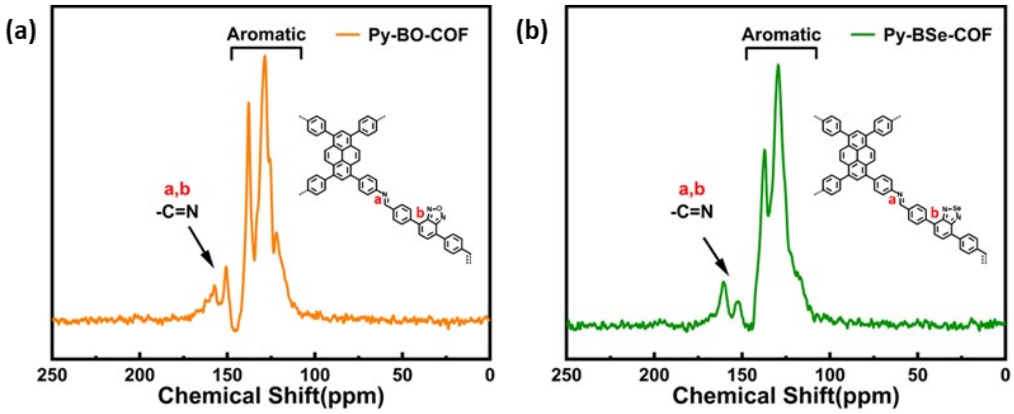

Fig. S8. Solid state ^{13}C CP/MAS NMR spectra of (a) Py-BO-COF and (b) Py-BSe-COF.

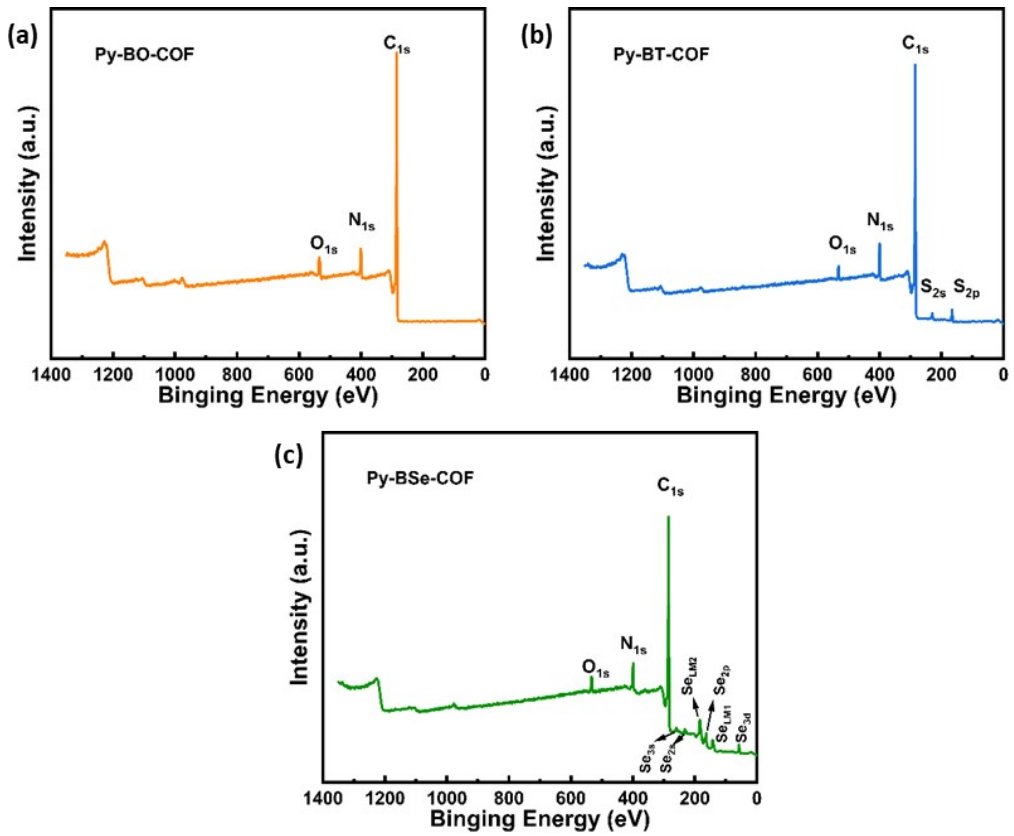

Fig. S9. XPS survey spectra of (a) Py-BO-COF, (b) Py-BT-COF and (c) Py-BSe-COF.

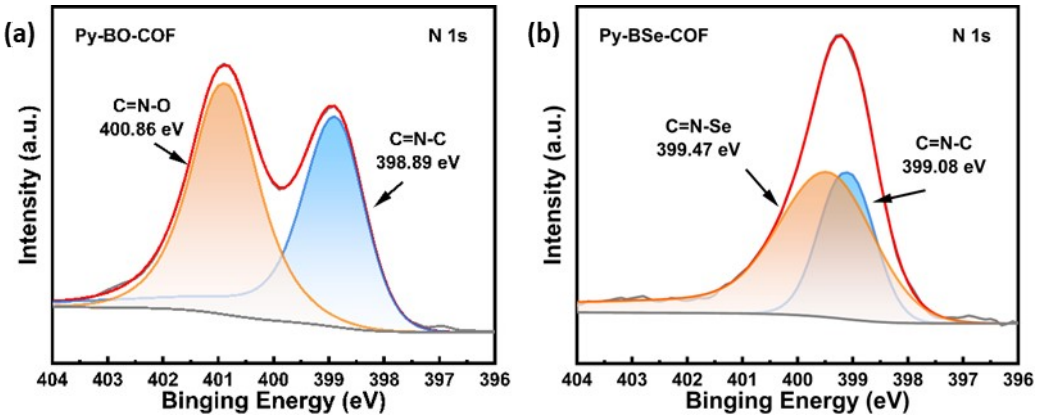

Fig. S10. High resolution XPS spectra of N 1s for (a) Py-BO-COF, (b) Py-BSe-COF.

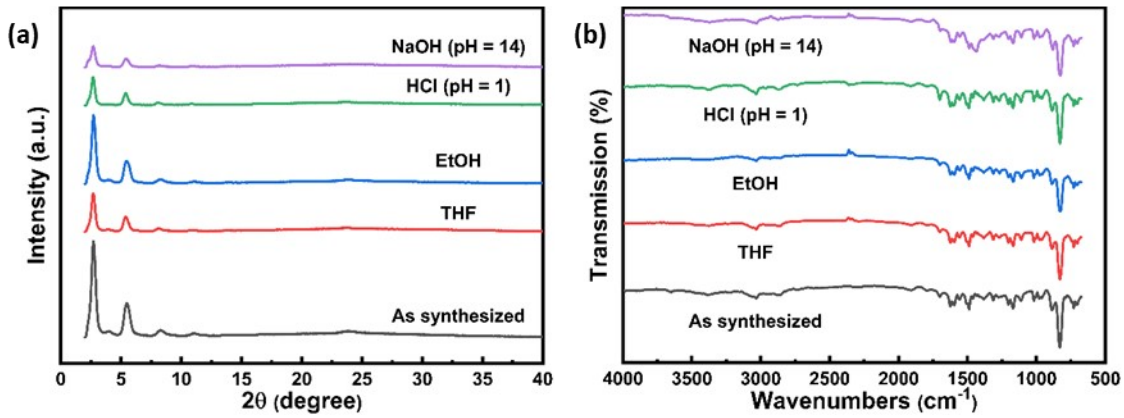

Fig. S11. (a) PXRD pattern and (b) FT-IR spectra of Py-BO-COF after various treatments for 24 h.

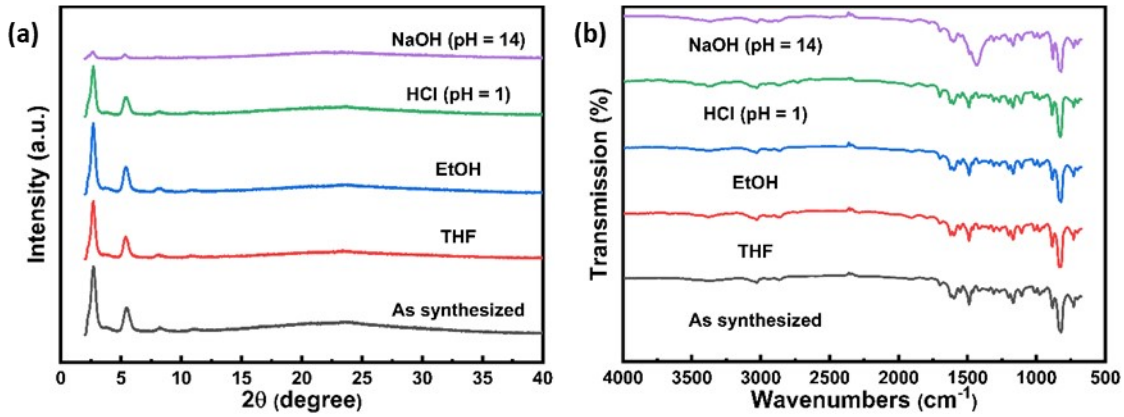

Fig. S12. (a) PXRD pattern and (b) FT-IR spectra of Py-BT-COF after various treatments for 24 h.

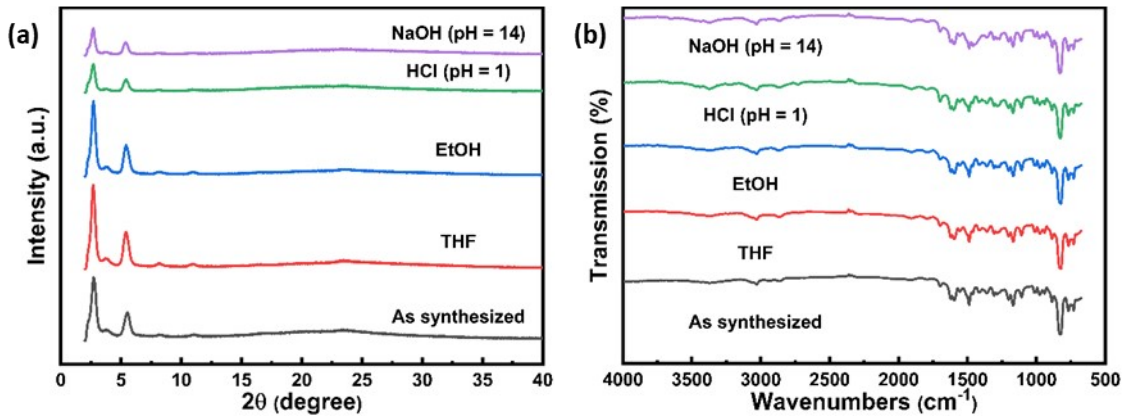

Fig. S13. (a) PXRD pattern and (b) FT-IR spectra of Py-BSe-COF after various treatments for 24 h.

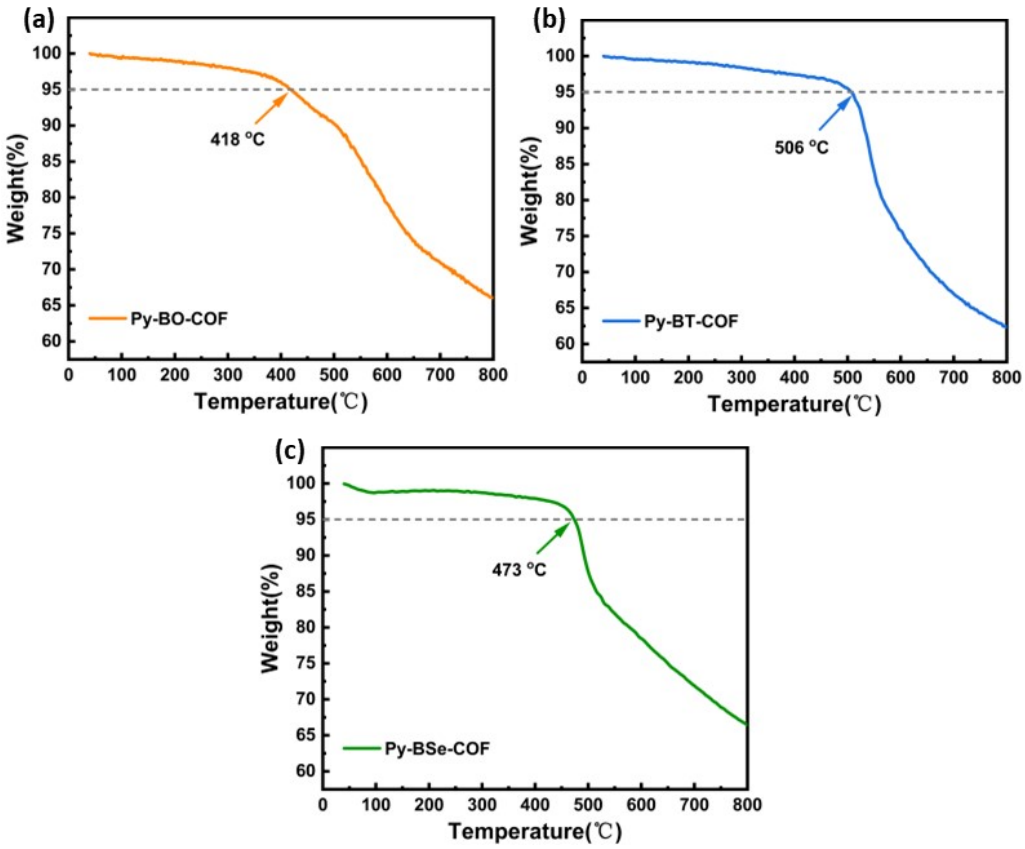

Fig. S14. TGA profiles of (a)Py-BO-COF, (b)Py-BT-COF and (c)Py-BSe-COF.

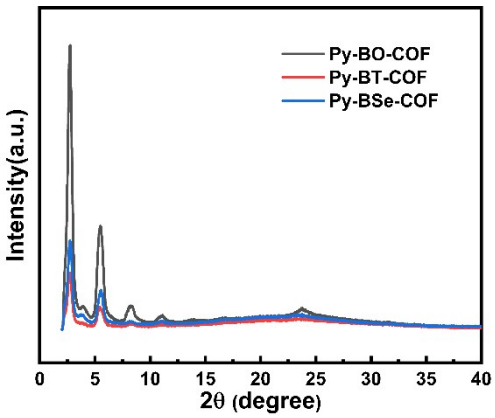

Fig. S15. PXRD patterns of Py-BO-COF, Py-BT-COF and Py-BSe-COF.

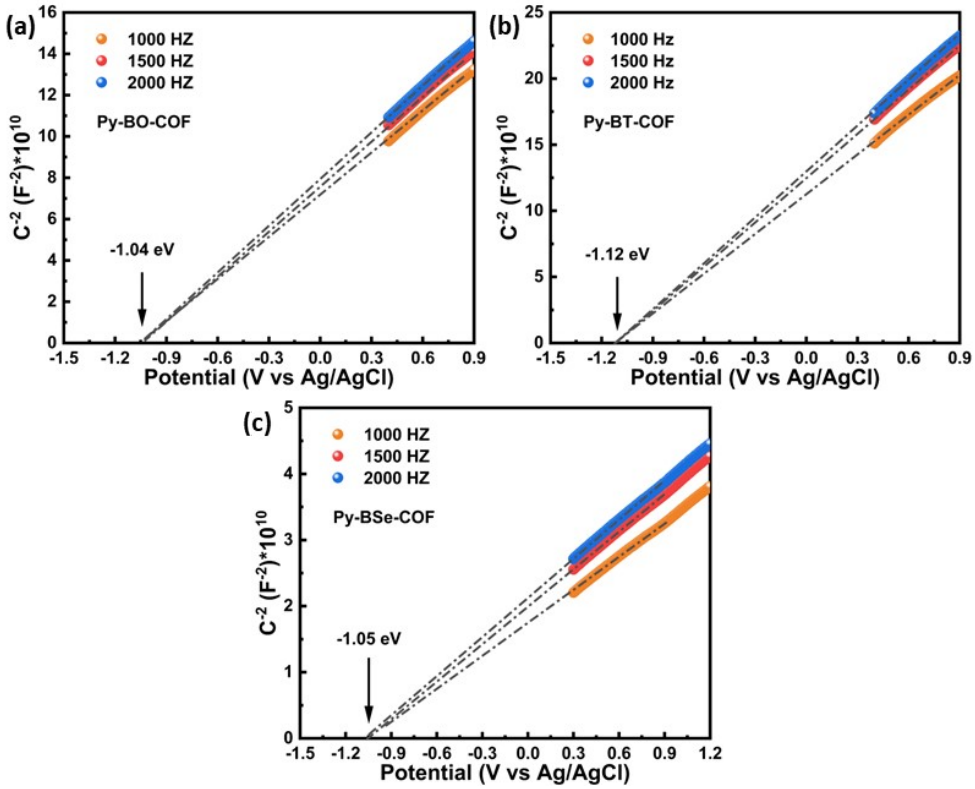

Fig. S16. Mott-Schottky (M-S) plot for (a)Py-BO-COF, (b)Py-BT-COF and (c)Py-BSe-COF measured in Na_2SO_4 (0.2 M, pH = 6.8) with Ag/AgCl electrode as the reference electrode in dark.

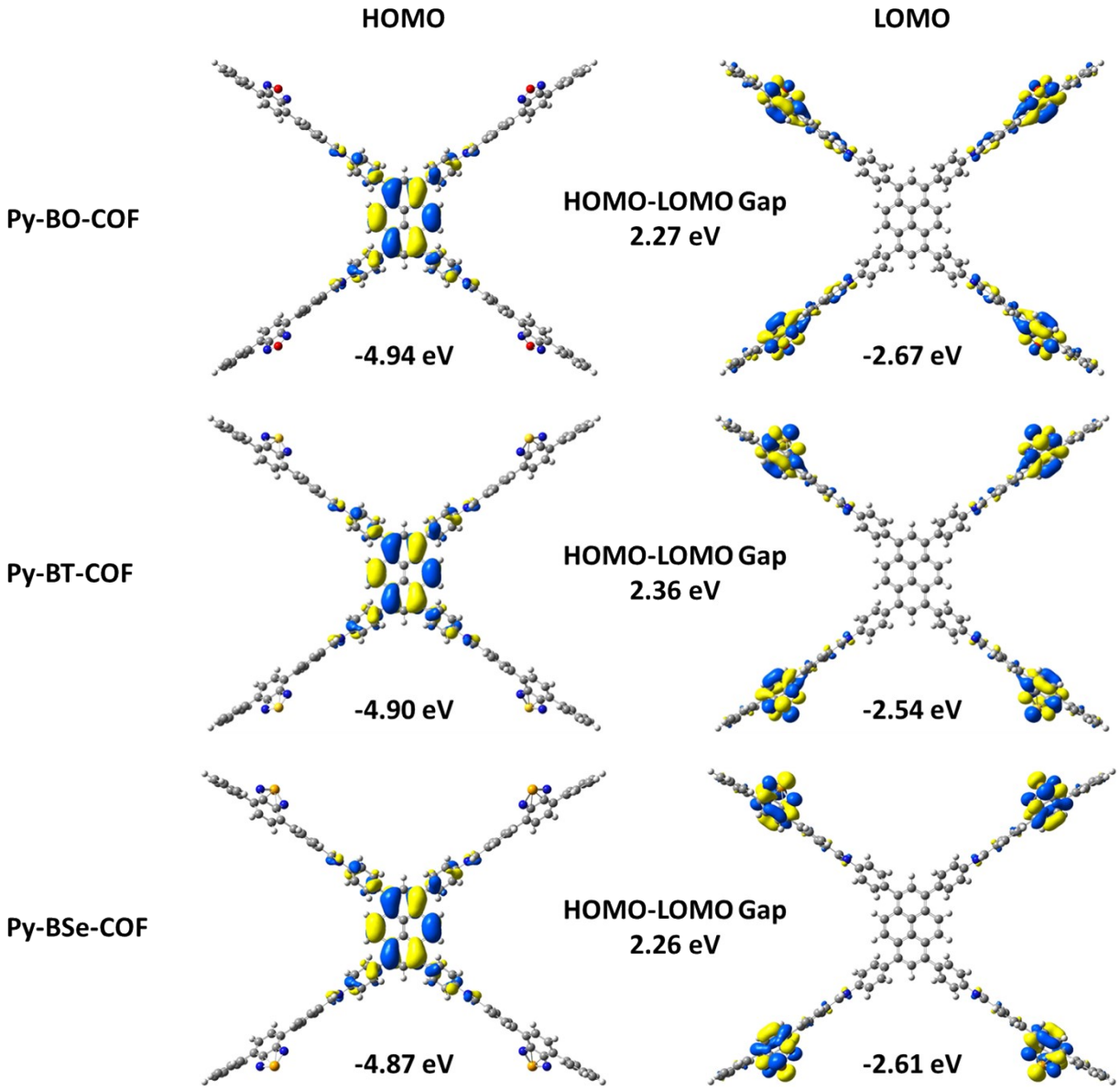

Fig. S17. HOMO and LUMO orbital distribution based on the fragments of Py-BO-COF, Py-BT-COF and Py-BSe-COF.

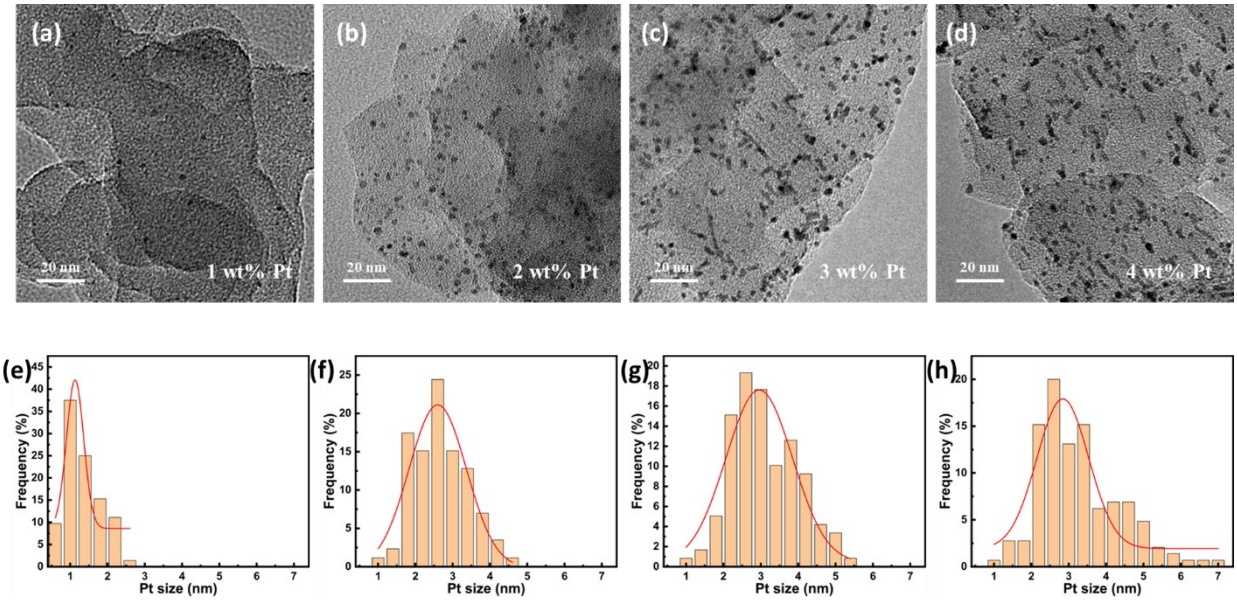

Fig. S18. HR-TEM images and photodeposited NPs size distributions of Py-BO-COF, at the Pt content of 1wt%(a, e), 2wt%(b, f), 3wt%(c, g), 4wt%(d, h).

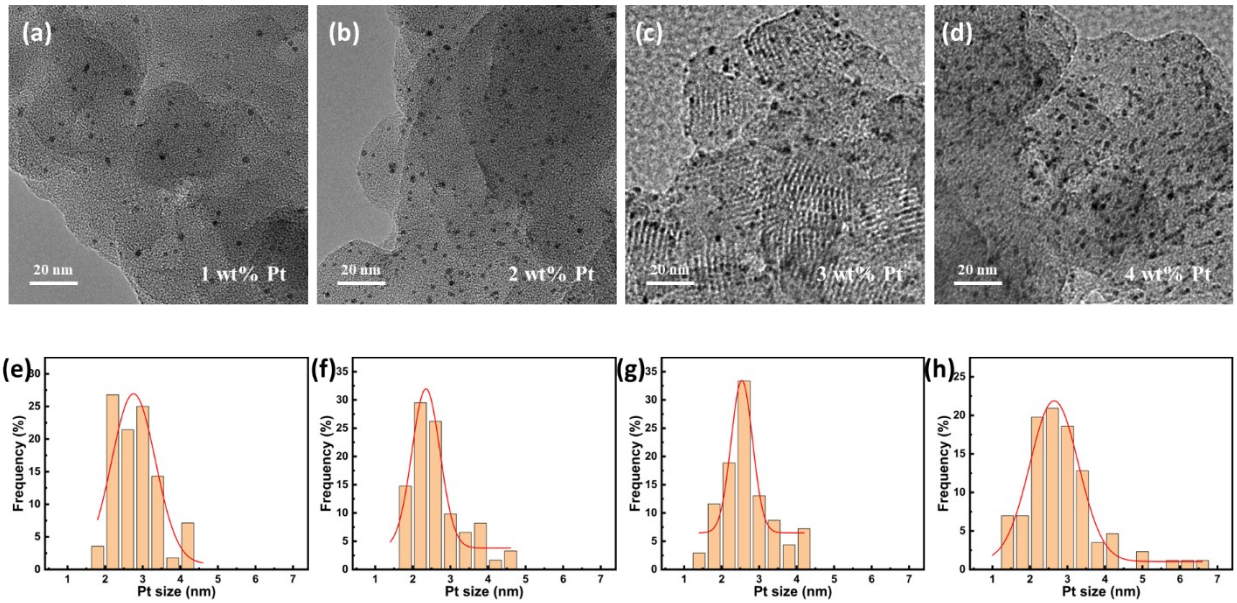

Fig. S19. HR-TEM images and photodeposited NPs size distributions of Py-BT-COF, at the Pt content of 1wt%(a, e), 2wt%(b, f), 3wt%(c, g), 4wt%(d, h).

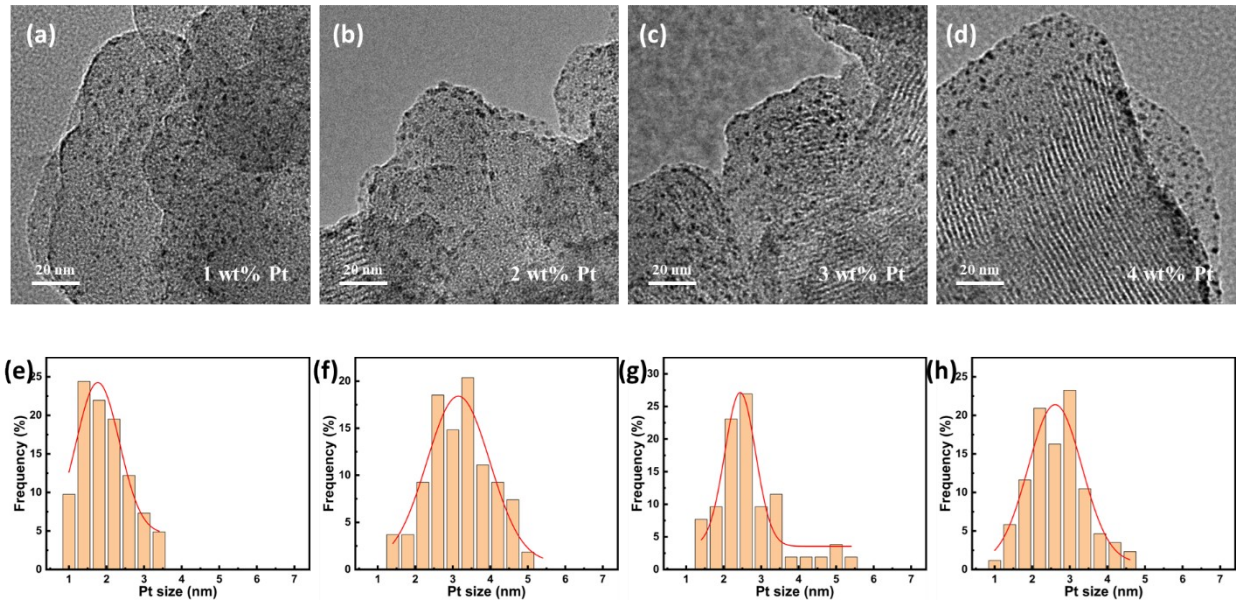

Fig. S20. HR-TEM images and photodeposited NPs size distributions of Py-BSe-COF, at the Pt content of 1wt%(a, e), 2wt%(b, f), 3wt%(c, g), 4wt%(d, h).

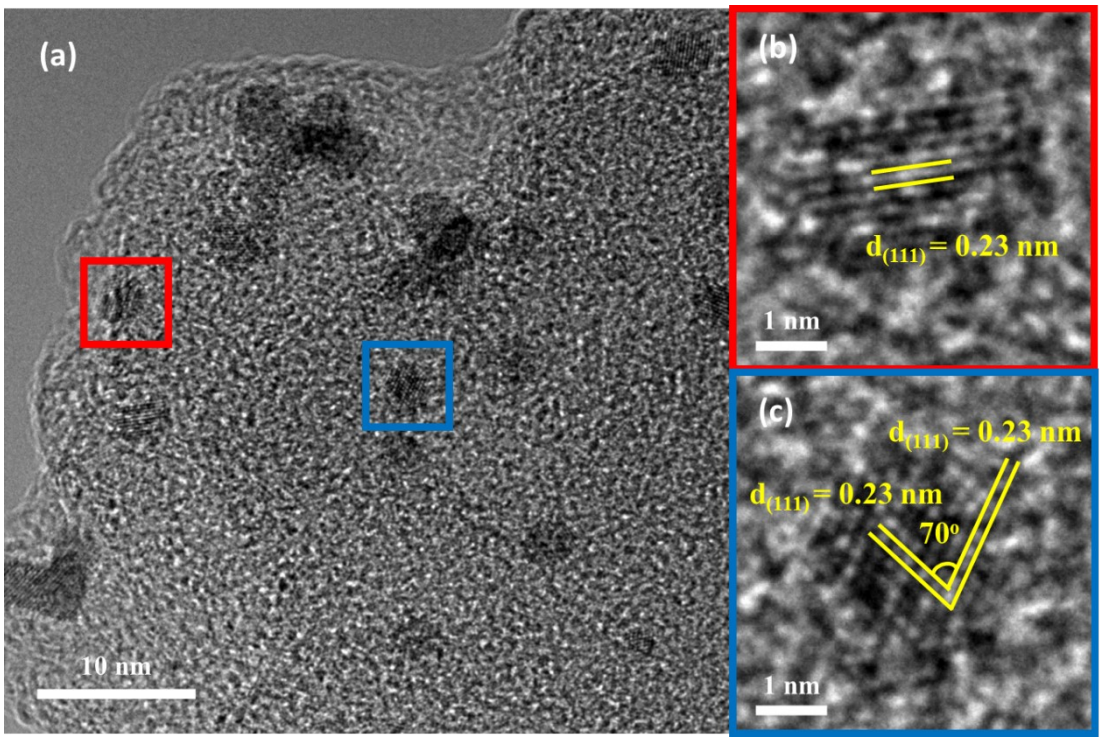

Fig. S21. (a)HR-TEM image of Pt NPs on Py-BO-COF. (b) Enlarged HR-TEM image of the red square area in (a). (c) Enlarged HR-TEM image of the blue square area in (a).

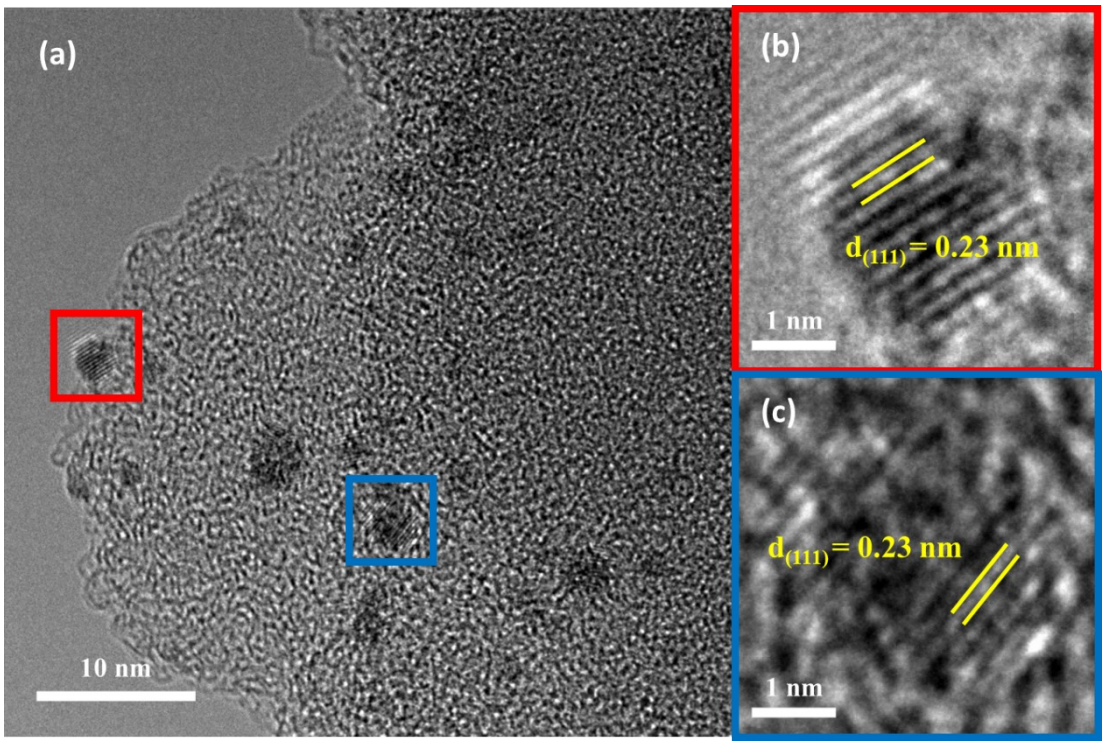

Fig. S22. (a)HR-TEM image of Pt NPs on Py-BT-COF. (b) Enlarged HR-TEM image of the red square area in (a). (c) Enlarged HR-TEM image of the blue square area in (a).

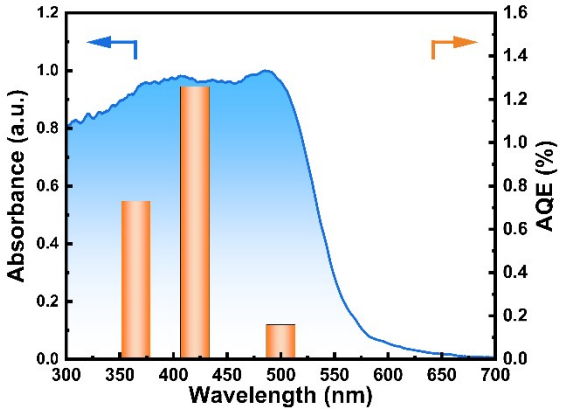

Fig. S23. Wavelength-dependent AQE of photocatalytic hydrogen evolution by Py-BT-COF.

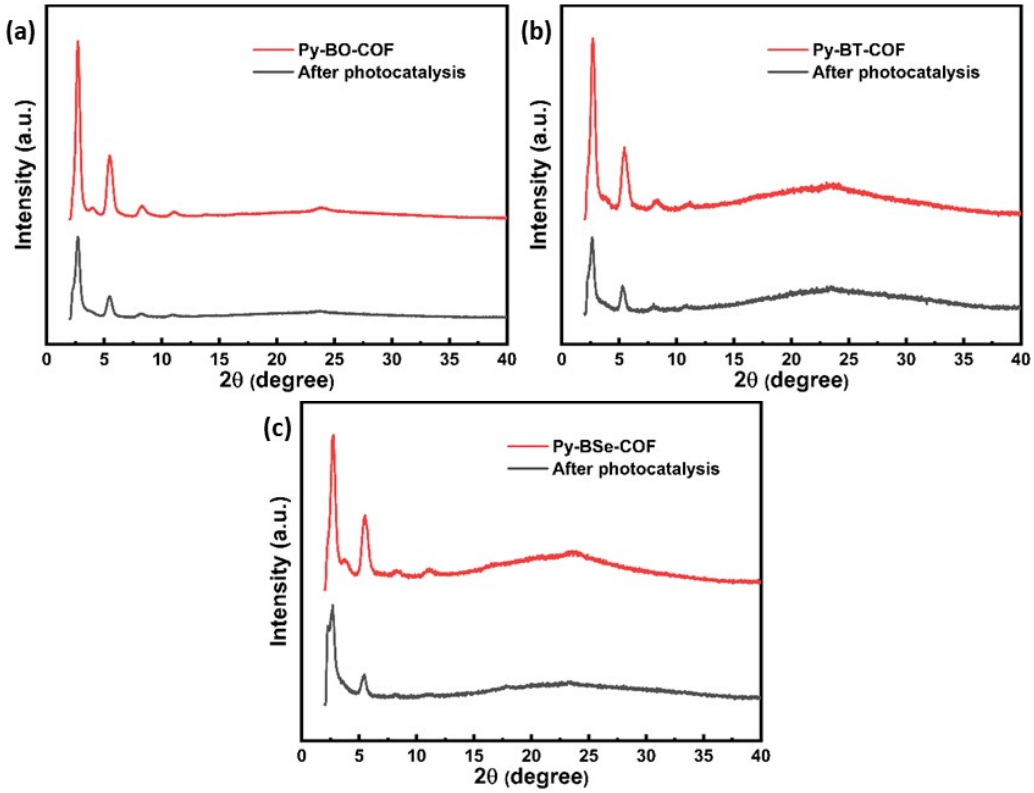

Fig. S24. PXRD patterns of (a)Py-BO-COF, (b)Py-BT-COF and (c)Py-BSe-COF before and after photocatalysis.

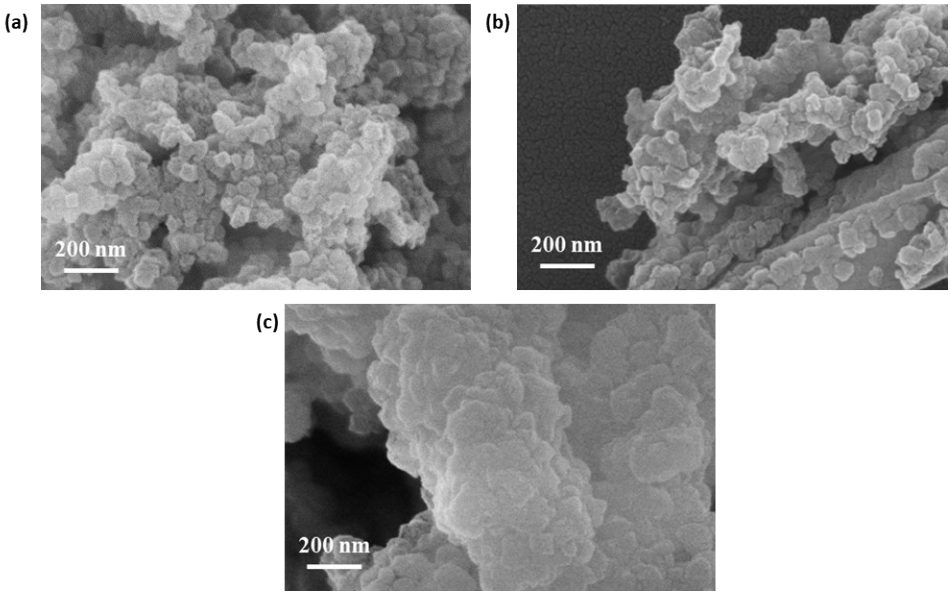

Fig. S25. SEM images of (a)Py-BO-COF, (b)Py-BT-COF and (c)Py-BSe-COF after photocatalysis.

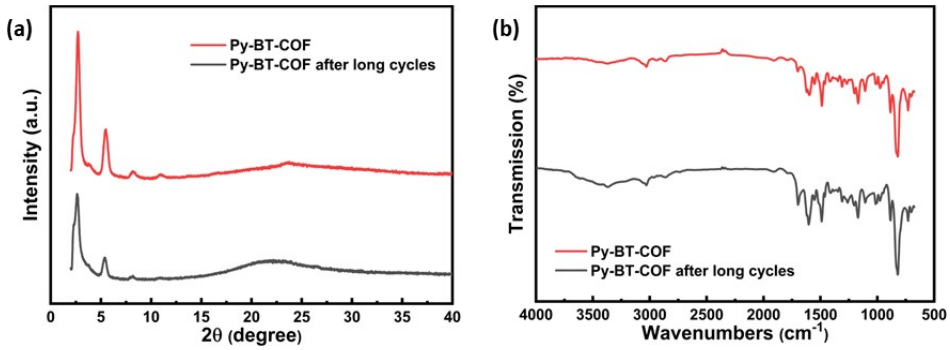

Fig. S26. (a)PXRD patterns and (b)FT-IR spectra of Py-BT-COF before and after of long cycles.

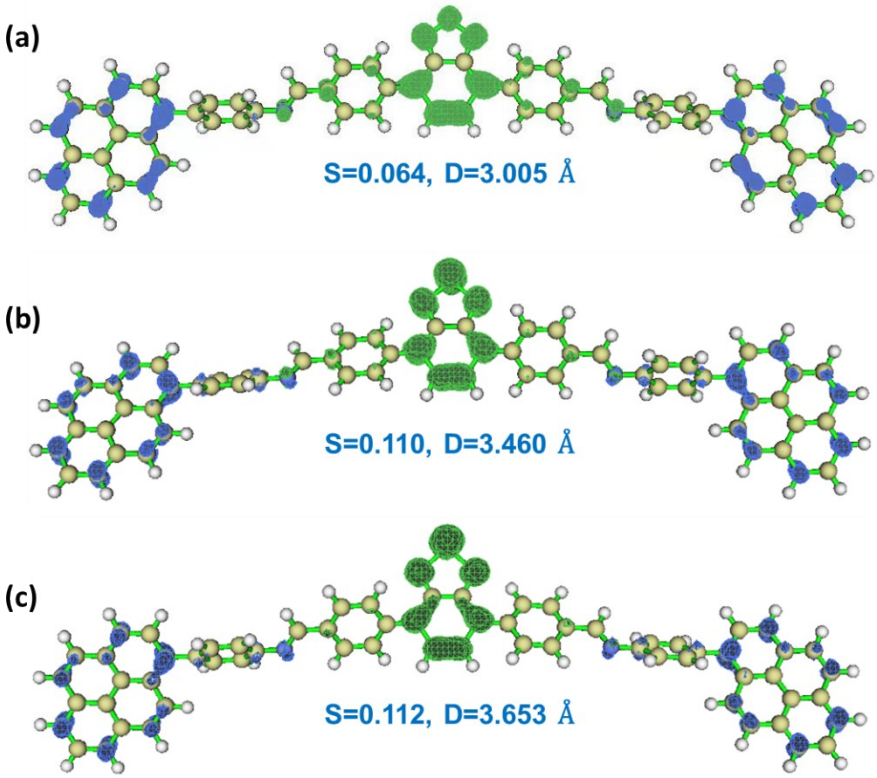

Fig. S27. The hole (blue) and electron (green) distribution of S1 excited state on (a)Py-BO-COF, (b)Py-BT-COF and (c)Py-BSe-COF. S is the overlap integral of hole-electron distribution and D means the distance between centroid of hole and electron. The balls in different colors represent different atoms: H, white; C, light yellow; N, blue; O, red; S, yellow; Se, orange.

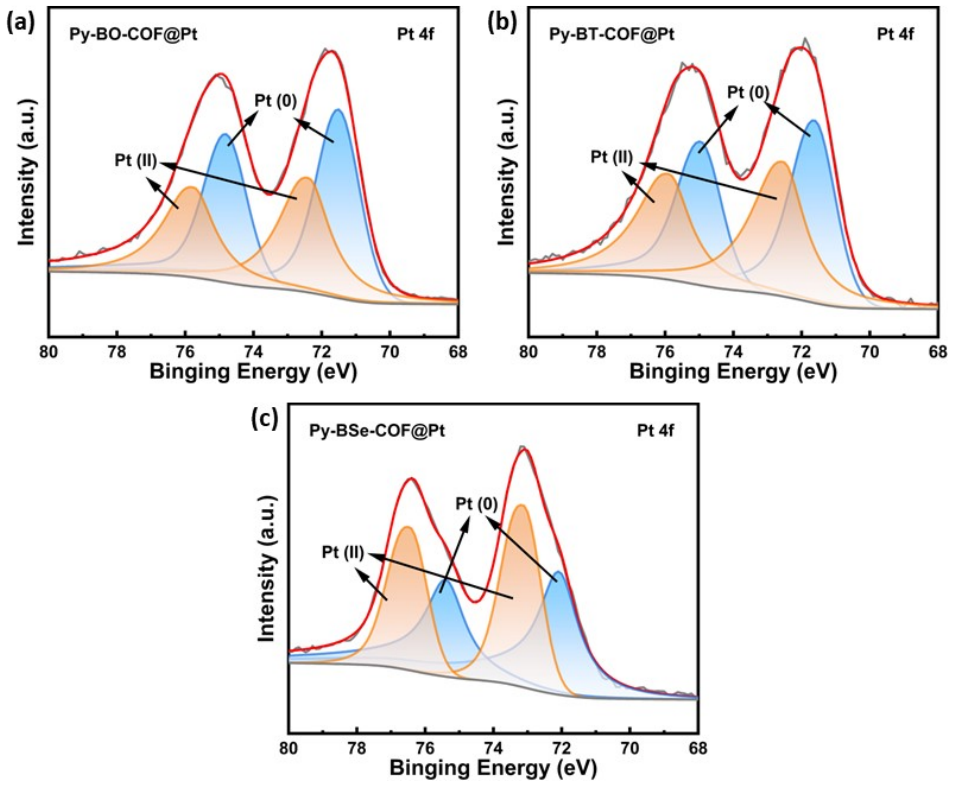

Fig. S28. High resolution XPS spectra of Pt 4f for (a)Py-BO-COF, (b)Py-BT-COF and (c)Py-BSe-COF after photocatalysis.

Table S1. Comparison of photocatalytic hydrogen evolution performance of benzothiadiazol-based COFs

Photocatalyst (amount)	Co-catalyst	Sacrificial reagent	Irradiation condition	AQE[a] (wavelength)	HER ($mmol \cdot g^{-1} \cdot h^{-1}$)	Reference
BT-TAPT-COF	Pt (8 wt% H_2PtCl_6)	0.1M AA[b]	λ＞420 nm	0.19 (410 nm)	0.95	[6]
HBT-COF (5 mg)	3 wt% Pt	0.1M AA	λ＞420 nm	-	3.8	[7]
BT-COF (5 mg)	3 wt% Pt	0.1M AA	λ＞420 nm	-	0.68	
HIAM-0004	5 wt% Pt	0.1M AA	λ＞420 nm	-	1.53	[8]
NKCOF-108 (10 mg)	5 wt% Pt	0.1M AA	λ＞420 nm	2.96 % (520 nm)	11.6	[9]
Py-ClTP-BTCOF (20 mg)	5 wt% Pt	0.1M AA	λ＞420 nm	8.45 % (420 nm)	8.87	[10]
Py-FTP-BTCOF (20 mg)	5 wt% Pt	0.1M AA	λ＞420 nm	-	2.87	
Py-HTP-BTCOF (20 mg)	5 wt% Pt	0.1M AA	λ＞420 nm	-	1.08	
COF-F (5 mg)	3 wt% Pt	0.1M AA	AM 1.5 G	0.29 % (500 nm)	10.58	[2]
COF-Cl (5 mg)	3 wt% Pt	0.1M AA	AM 1.5 G	-	5.84	
COF-H (5 mg)	3 wt% Pt	0.1M AA	AM 1.5 G	-	5.03	
Py-BT-COF (5 mg)	2 wt% Pt	0.1M AA	AM 1.5 G	1.26 % (420 nm)	10.00	This work

a. AQE: apparent quantum efficiency. **b.** AA: Ascorbic acid.

Table S2. Comparison of photocatalytic hydrogen evolution performance of pyrene-based COFs

Photocatalyst (amount)	Co-catalyst	Sacrificial reagent	Irradiation condition	AQE[a] (wavelength)	HER ($mmol \cdot g^{-1} \cdot h^{-1}$)	Reference
$sp^2c\text{-}COF_{ERDN}$ (50 mg)	5 wt% Pt	10 vol% TEOA[b]	λ＞420 nm	0.48 % (495 nm)	2.12	[11]
sp^2c-COF (50 mg)	3 wt% Pt	10 vol% TEOA	λ＞420 nm	-	1.36	
PyTz-COF (35 mg)	3 wt% Pt	0.1M AA[c]	AM 1.5 G	-	2.07	[12]
Py-ClTP-BTCOF (20 mg)	5 wt% Pt	0.1M AA	λ＞420 nm	8.45 % (420 nm)	8.87	[10]
Py-FTP-BTCOF (20 mg)	5 wt% Pt	0.1M AA	λ＞420 nm	-	2.87	
Py-HTP-BTCOF (20 mg)	5 wt% Pt	0.1M AA	λ＞420 nm	-	1.08	
NKCOF-108 (10 mg)	5 wt% Pt	0.1M AA	λ＞420 nm	2.96 % (520 nm)	11.6	[9]
Py-BT-COF (5 mg)	2 wt% Pt	0.1M AA	AM 1.5 G	1.26 % (420 nm)	10.00	This work
Py-BO-COF (5 mg)	2 wt% Pt	0.1M AA	AM 1.5 G	-	5.47	
Py-BSe-COF (5 mg)	2 wt% Pt	0.1M AA	AM 1.5 G	-	0.12	

a. AQE: apparent quantum efficiency. **b.** TEOA: triethanolamine. **c.** AA: Ascorbic acid.

Table S3. Atomic coordinates of the simulated Py-BO-COF based on AA-stacking mode.

Space group		**P1**	
Cell parameters		**a = 32.8332, b = 32.7660, c = 3.8223 α = 100.343, β = 99.6302, γ = 80.1542**	
atoms	**x**	**y**	**z**
C1	-0.42978	-0.2779	0.43172
C2	-0.43528	-0.31755	0.50162
C3	-0.40137	-0.3511	0.49836
C4	-0.36211	-0.34486	0.42537
C5	-0.35872	-0.30649	0.32589
C6	-0.39177	-0.27379	0.32884
C7	-0.46286	-0.24388	0.4562
C8	-0.50199	-0.25157	0.50744
C9	-0.5089	-0.2911	0.5562
C10	-0.47454	-0.32379	0.57462
C11	-0.40686	-0.39075	0.56823
C12	-0.44488	-0.39484	0.67129
C13	-0.47794	-0.36214	0.67417
C14	-0.32774	-0.37756	0.44384
C15	-0.33466	-0.4171	0.49214
C16	-0.3738	-0.42478	0.54334
C17	-0.28393	-0.37149	0.42888
C18	-0.45773	-0.19968	0.44305
C19	-0.55272	-0.29709	0.57194
C20	-0.37901	-0.46898	0.55567
C21	-0.42312	-0.18209	0.64219
C22	-0.4192	-0.14035	0.6391
C23	-0.45016	-0.11477	0.4478
C24	-0.48542	-0.13177	0.25513
C25	-0.48908	-0.17369	0.25387
C26	-0.26726	-0.33632	0.63138
C27	-0.22588	-0.33135	0.62821
C28	-0.19981	-0.3621	0.42836
C29	-0.21579	-0.39782	0.23779
C30	-0.25734	-0.40254	0.23644
C31	-0.41372	-0.4864	0.35675
C32	-0.4179	-0.52804	0.36054
C33	-0.3871	-0.55372	0.5524
C34	-0.35163	-0.53697	0.74349
C35	-0.34772	-0.4951	0.7443

C36	-0.56952	-0.3322	0.36956
C37	-0.611	-0.33693	0.37208
C38	-0.63698	-0.306	0.5712
C39	-0.62084	-0.2704	0.76224
C40	-0.57921	-0.26594	0.7643
N41	-0.44402	-0.07222	0.45467
C42	-0.47018	-0.04295	0.31479
C43	-0.45926	-0.00043	0.34732
N44	-0.157	-0.35888	0.41534
C45	-0.13878	-0.32571	0.52603
C46	-0.09416	-0.32711	0.50147
N47	-0.39368	-0.59609	0.54755
C48	-0.36834	-0.62521	0.69639
C49	-0.37996	-0.66743	0.66539
N50	-0.67996	-0.30881	0.58099
C51	-0.69827	-0.34198	0.47494
C52	-0.74312	-0.34003	0.49386
C53	-0.48936	0.03165	0.22474
C54	-0.47994	0.07236	0.26174
C55	-0.44011	0.08165	0.41925
C56	-0.40973	0.04935	0.53561
C57	-0.41928	0.00872	0.50201
C58	-0.07477	-0.29152	0.64119
C59	-0.03231	-0.2925	0.62903
C60	-0.00839	-0.32919	0.47868
C61	-0.02798	-0.36458	0.33245
C62	-0.0705	-0.36358	0.34402
C63	-0.3508	-0.6995	0.79954
C64	-0.36104	-0.73988	0.76607
C65	-0.40072	-0.74875	0.59964
C66	-0.43012	-0.71651	0.47081
C67	-0.41976	-0.67627	0.50138
C68	-0.76251	-0.37581	0.36452
C69	-0.8052	-0.37428	0.37088
C70	-0.8294	-0.33682	0.50444
C71	-0.80973	-0.30121	0.63997
C72	-0.76701	-0.30281	0.63521
C73	-0.41134	-0.79161	0.55841
C74	-0.87512	-0.33443	0.4946
C75	-0.38385	-0.82701	0.44038
C76	-0.39282	-0.866	0.39883
C77	-0.43063	-0.87491	0.46796
C78	-0.45963	-0.84009	0.58799

C79	-0.45011	-0.79881	0.63201
C80	-0.89304	-0.36719	0.56899
C81	-0.93414	-0.36534	0.56253
C82	-0.96304	-0.33065	0.4786
C83	-0.9466	-0.29663	0.40049
C84	-0.90313	-0.29856	0.40707
N85	-0.36109	-0.89177	0.26333
O86	-0.33304	-0.86931	0.22222
N87	-0.34686	-0.82958	0.3287
N88	-0.94018	-0.40029	0.66962
O89	-0.90371	-0.42347	0.73846
N90	-0.87472	-0.40333	0.67852
H91	-0.33074	-0.30159	0.23584
H92	-0.38743	-0.24555	0.24048
H93	-0.52773	-0.22613	0.50925
H94	-0.44923	-0.42307	0.75974
H95	-0.50592	-0.36704	0.76425
H96	-0.30893	-0.44255	0.49
H97	-0.39936	-0.2004	0.80518
H98	-0.39232	-0.12736	0.79292
H99	-0.50988	-0.11348	0.09933
H100	-0.51639	-0.18585	0.10112
H101	-0.286	-0.31295	0.79845
H102	-0.21436	-0.30419	0.79231
H103	-0.1959	-0.42174	0.08477
H104	-0.26868	-0.43036	0.08221
H105	-0.43742	-0.46802	0.19398
H106	-0.44492	-0.54086	0.20749
H107	-0.32719	-0.55542	0.89803
H108	-0.32032	-0.48308	0.89652
H109	-0.55085	-0.35564	0.20248
H110	-0.62273	-0.36396	0.20744
H111	-0.64067	-0.24635	0.91464
H112	-0.56778	-0.23815	0.91841
H113	-0.5007	-0.04867	0.17808
H114	-0.15581	-0.29632	0.63675
H115	-0.33818	-0.61951	0.84191
H116	-0.68113	-0.37172	0.37269
H117	-0.52026	0.02522	0.10163
H118	-0.50363	0.09656	0.16368
H119	-0.37882	0.05577	0.65941
H120	-0.3956	-0.01555	0.59905
H121	-0.09237	-0.26312	0.76482

H122	-0.0179	-0.26488	0.74516
H123	-0.01034	-0.3929	0.20692
H124	-0.08501	-0.39122	0.23005
H125	-0.32005	-0.69332	0.92963
H126	-0.33818	-0.76422	0.87335
H127	-0.46077	-0.72273	0.33911
H128	-0.44269	-0.65204	0.39464
H129	-0.74473	-0.40484	0.25358
H130	-0.81952	-0.40219	0.26326
H131	-0.82738	-0.27221	0.75235
H132	-0.75255	-0.27498	0.74114
H133	-0.48919	-0.8448	0.6531
H134	-0.47263	-0.77276	0.72805
H135	-0.96726	-0.26896	0.32932
H136	-0.89158	-0.27243	0.3377

Table S4. Atomic coordinates of the simulated Py-BT-COF based on AA-stacking mode.

Space group		**P1**	
Cell parameters		**a = 32.8433, b = 32.7698, c = 3.8300 α = 99.4459, β = 97.9068, γ = 81.7388**	
atoms	**x**	**y**	**z**
C1	-0.43039	-0.27716	0.42609
C2	-0.43612	-0.31679	0.50124
C3	-0.40267	-0.34971	0.49372
C4	-0.36362	-0.34284	0.41147
C5	-0.35995	-0.30449	0.30804
C6	-0.39258	-0.27243	0.31474
C7	-0.46303	-0.24379	0.45445
C8	-0.50194	-0.25207	0.51566
C9	-0.50907	-0.29159	0.56994
C10	-0.47517	-0.32366	0.58365
C11	-0.40839	-0.38934	0.56883
C12	-0.44621	-0.39407	0.68026
C13	-0.47883	-0.362	0.68723
C14	-0.32971	-0.37489	0.42532
C15	-0.33684	-0.41443	0.47933
C16	-0.37576	-0.42271	0.54043
C17	-0.28613	-0.36813	0.40158
C18	-0.45762	-0.19965	0.43551
C19	-0.55263	-0.29831	0.59493

C20	-0.38118	-0.46686	0.55899
C21	-0.42321	-0.18165	0.62538
C22	-0.41902	-0.13998	0.61753
C23	-0.44948	-0.11491	0.43008
C24	-0.4846	-0.13231	0.24746
C25	-0.48852	-0.17418	0.25076
C26	-0.26936	-0.33306	0.5994
C27	-0.22797	-0.32781	0.5935
C28	-0.20202	-0.35817	0.3951
C29	-0.2183	-0.39353	0.20531
C30	-0.25983	-0.39855	0.20724
C31	-0.41558	-0.48483	0.36874
C32	-0.41975	-0.52653	0.37542
C33	-0.38928	-0.55165	0.5623
C34	-0.35416	-0.53428	0.74526
C35	-0.35027	-0.49238	0.74324
C36	-0.56949	-0.3334	0.39819
C37	-0.61081	-0.33869	0.40683
C38	-0.63659	-0.30836	0.60705
C39	-0.6203	-0.27289	0.79437
C40	-0.57884	-0.26784	0.78983
N41	-0.44315	-0.07233	0.43384
C42	-0.46787	-0.04397	0.28214
C43	-0.45687	-0.00126	0.31572
N44	-0.15896	-0.35517	0.38527
C45	-0.13935	-0.32323	0.51458
C46	-0.0945	-0.32531	0.49547
N47	-0.39549	-0.59432	0.55581
C48	-0.37113	-0.62253	0.71247
C49	-0.38184	-0.66541	0.67386
N50	-0.67952	-0.31155	0.6209
C51	-0.69854	-0.34422	0.50661
C52	-0.74329	-0.34254	0.52845
C53	-0.4858	0.03001	0.18332
C54	-0.4763	0.07087	0.22106
C55	-0.43756	0.08111	0.38917
C56	-0.40837	0.04964	0.51637
C57	-0.418	0.00887	0.48163
C58	-0.07358	-0.29146	0.65902
C59	-0.03083	-0.29343	0.65673
C60	-0.0082	-0.32938	0.49221
C61	-0.02928	-0.36288	0.32063
C62	-0.07207	-0.36092	0.32291

C63	-0.3532	-0.69645	0.81304
C64	-0.3624	-0.73747	0.77067
C65	-0.40047	-0.74807	0.5895
C66	-0.42942	-0.71686	0.45601
C67	-0.42011	-0.67593	0.49604
C68	-0.76355	-0.37738	0.38236
C69	-0.80619	-0.37595	0.38894
C70	-0.82943	-0.33956	0.54057
C71	-0.80892	-0.30495	0.69292
C72	-0.76625	-0.30643	0.6873
C73	-0.40998	-0.79163	0.53803
C74	-0.87509	-0.33705	0.53063
C75	-0.3814	-0.82523	0.4151
C76	-0.39006	-0.86545	0.36772
C77	-0.4281	-0.87526	0.43816
C78	-0.45744	-0.84197	0.55969
C79	-0.4485	-0.8006	0.60854
C80	-0.89422	-0.37	0.60241
C81	-0.93628	-0.36752	0.59017
C82	-0.96262	-0.33201	0.50365
C83	-0.94422	-0.29842	0.43239
C84	-0.90099	-0.30096	0.44454
N85	-0.35939	-0.89302	0.24002
S86	-0.31897	-0.86928	0.17836
N87	-0.34417	-0.822	0.32248
N88	-0.94858	-0.40144	0.67807
S89	-0.90787	-0.43746	0.77254
N90	-0.87441	-0.40594	0.69793
H91	-0.33206	-0.2991	0.21248
H92	-0.38804	-0.24416	0.22312
H93	-0.52735	-0.22711	0.52081
H94	-0.45074	-0.42234	0.77181
H95	-0.5067	-0.36737	0.78323
H96	-0.31143	-0.43938	0.47417
H97	-0.39982	-0.19958	0.78501
H98	-0.39231	-0.12664	0.76458
H99	-0.50886	-0.11431	0.09771
H100	-0.51568	-0.18669	0.10559
H101	-0.288	-0.31008	0.76629
H102	-0.21646	-0.30075	0.75472
H103	-0.19855	-0.4171	0.0527
H104	-0.27133	-0.42622	0.05555
H105	-0.43898	-0.46686	0.20951

H106	-0.44644	-0.53984	0.22774
H107	-0.3298	-0.55237	0.89334
H108	-0.32309	-0.47989	0.88851
H109	-0.55096	-0.35636	0.23017
H110	-0.62249	-0.36569	0.24589
H111	-0.63994	-0.24932	0.94801
H112	-0.5673	-0.24014	0.94033
H113	-0.49713	-0.05064	0.13297
H114	-0.15516	-0.29463	0.64235
H115	-0.34241	-0.61557	0.87015
H116	-0.6822	-0.37326	0.3919
H117	-0.51582	0.02283	0.05162
H118	-0.49904	0.09445	0.11535
H119	-0.37836	0.0568	0.6488
H120	-0.39525	-0.01475	0.58681
H121	-0.09022	-0.26378	0.79483
H122	-0.01523	-0.26729	0.79185
H123	-0.01252	-0.39049	0.18392
H124	-0.08772	-0.38717	0.19059
H125	-0.32366	-0.68898	0.95381
H126	-0.33996	-0.76101	0.88169
H127	-0.45882	-0.72441	0.31305
H128	-0.44258	-0.65252	0.38492
H129	-0.7465	-0.40552	0.25734
H130	-0.82117	-0.40304	0.26791
H131	-0.82591	-0.27683	0.81835
H132	-0.75112	-0.27937	0.8062
H133	-0.48694	-0.84806	0.62319
H134	-0.47134	-0.77567	0.70721
H135	-0.96333	-0.27054	0.36113
H136	-0.88783	-0.27506	0.37961

Table S5. Atomic coordinates of the simulated Py-BSe-COF based on AA-stacking mode.

Space group		**P1**	
Cell parameters		**a = 32.9060, b = 32.8144, c = 3.8831 α = 99.4459, β = 97.9068, γ = 81.7388**	
atoms	**x**	**y**	**z**
C1	-0.43058	-0.27674	0.54051
C2	-0.43604	-0.31595	0.46613
C3	-0.40192	-0.34967	0.45425

C4	-0.3625	-0.34411	0.51798
C5	-0.35922	-0.3063	0.62435
C6	-0.39247	-0.27334	0.6345
C7	-0.46382	-0.24248	0.52956
C8	-0.50321	-0.24957	0.48924
C9	-0.5101	-0.28878	0.43825
C10	-0.4755	-0.32159	0.40431
C11	-0.40743	-0.38887	0.37984
C12	-0.44564	-0.39237	0.28849
C13	-0.47894	-0.35951	0.30113
C14	-0.32791	-0.37697	0.48421
C15	-0.33483	-0.41605	0.42959
C16	-0.3742	-0.42312	0.38945
C17	-0.28395	-0.37171	0.49391
C18	-0.45843	-0.19861	0.54471
C19	-0.55414	-0.2946	0.43921
C20	-0.37964	-0.46703	0.37563
C21	-0.42361	-0.18137	0.33694
C22	-0.41923	-0.13997	0.34337
C23	-0.44985	-0.11444	0.54833
C24	-0.48545	-0.13102	0.74862
C25	-0.48961	-0.17262	0.74589
C26	-0.26672	-0.33634	0.30104
C27	-0.22528	-0.33208	0.30443
C28	-0.19972	-0.36397	0.48891
C29	-0.21598	-0.39996	0.66696
C30	-0.25775	-0.4037	0.67351
C31	-0.4143	-0.48431	0.58612
C32	-0.4185	-0.52586	0.58364
C33	-0.38785	-0.5515	0.37979
C34	-0.35244	-0.53484	0.17643
C35	-0.3485	-0.49309	0.17489
C36	-0.57068	-0.32958	0.64577
C37	-0.6123	-0.33444	0.65863
C38	-0.63886	-0.3036	0.47237
C39	-0.62273	-0.26837	0.27246
C40	-0.58092	-0.26374	0.25608
N41	-0.44313	-0.07228	0.54412
C42	-0.46776	-0.04363	0.71252
C43	-0.45621	-0.00147	0.67651
N44	-0.15673	-0.36148	0.48959
C45	-0.14223	-0.32716	0.48687
C46	-0.0973	-0.32833	0.48944

N47	-0.39402	-0.59402	0.39221
C48	-0.3699	-0.62235	0.21689
C49	-0.38033	-0.66513	0.26583
N50	-0.682	-0.30666	0.47515
C51	-0.70296	-0.33577	0.65872
C52	-0.74736	-0.33489	0.63633
C53	-0.48509	0.03037	0.82817
C54	-0.47504	0.07075	0.78873
C55	-0.43577	0.07992	0.59908
C56	-0.4066	0.0478	0.45367
C57	-0.41679	0.00755	0.4899
C58	-0.08394	-0.29544	0.6
C59	-0.04156	-0.29699	0.61522
C60	-0.0113	-0.33094	0.50938
C61	-0.02493	-0.36301	0.38529
C62	-0.06745	-0.36207	0.38139
C63	-0.35145	-0.69655	0.10811
C64	-0.36025	-0.73755	0.16066
C65	-0.3982	-0.74773	0.3699
C66	-0.42744	-0.71615	0.52244
C67	-0.4185	-0.67524	0.4724
C68	-0.76873	-0.36706	0.8347
C69	-0.81101	-0.36657	0.82458
C70	-0.83282	-0.33443	0.60811
C71	-0.81108	-0.3021	0.40953
C72	-0.76896	-0.3022	0.42558
C73	-0.40693	-0.79141	0.43317
C74	-0.87757	-0.33495	0.583
C75	-0.37518	-0.82681	0.54261
C76	-0.38433	-0.86937	0.59881
C77	-0.42551	-0.87697	0.54862
C78	-0.45358	-0.8435	0.45159
C79	-0.44415	-0.79988	0.39348
C80	-0.8946	-0.37469	0.6217
C81	-0.93872	-0.3738	0.61225
C82	-0.96613	-0.33321	0.5362
C83	-0.94866	-0.298	0.4916
C84	-0.90423	-0.29885	0.52454
N85	-0.35544	-0.89838	0.70467
Se86	-0.30843	-0.87541	0.74887
N87	-0.33927	-0.82265	0.60636
N88	-0.95113	-0.40991	0.66923
Se89	-0.90635	-0.45404	0.73095

N90	-0.87276	-0.41153	0.66879
H91	-0.33124	-0.3021	0.70998
H92	-0.38827	-0.24547	0.72619
H93	-0.52915	-0.22398	0.49804
H94	-0.44996	-0.42029	0.19834
H95	-0.50717	-0.36392	0.22114
H96	-0.30897	-0.4417	0.41987
H97	-0.40005	-0.19972	0.16518
H98	-0.39218	-0.12723	0.18277
H99	-0.5099	-0.1126	0.91147
H100	-0.51713	-0.18454	0.90438
H101	-0.28512	-0.31222	0.14321
H102	-0.21272	-0.30474	0.15275
H103	-0.19624	-0.42474	0.80711
H104	-0.26948	-0.43166	0.81989
H105	-0.43783	-0.46591	0.75776
H106	-0.44536	-0.53865	0.7472
H107	-0.32783	-0.5534	0.01617
H108	-0.32107	-0.48117	0.01457
H109	-0.55154	-0.35307	0.80176
H110	-0.62318	-0.36206	0.81868
H111	-0.64278	-0.24461	0.12639
H112	-0.56953	-0.23615	0.09804
H113	-0.49728	-0.04966	0.87848
H114	-0.1633	-0.29774	0.50258
H115	-0.34154	-0.61558	0.03551
H116	-0.68875	-0.36107	0.83605
H117	-0.51549	0.02401	0.97631
H118	-0.49774	0.09477	0.90971
H119	-0.37613	0.05408	0.30628
H120	-0.39404	-0.01653	0.37013
H121	-0.10655	-0.26922	0.68678
H122	-0.03287	-0.2722	0.72183
H123	-0.00285	-0.38875	0.285
H124	-0.07707	-0.38729	0.28642
H125	-0.32198	-0.68939	-0.05448
H126	-0.33758	-0.76143	0.03628
H127	-0.4567	-0.72342	0.68789
H128	-0.44113	-0.65155	0.5983
H129	-0.75296	-0.39219	1.00502
H130	-0.82663	-0.39111	0.99451
H131	-0.82602	-0.27742	0.23093
H132	-0.75293	-0.2772	0.26737

H133	-0.48374	-0.84797	0.40548
H134	-0.46793	-0.77462	0.30978
H135	-0.96675	-0.26755	0.42509
H136	-0.89396	-0.26889	0.50444

Section IV. Supplementary References

1. T. Takata, J. Jiang, Y. Sakata, M. Nakabayashi, N. Shibata, V. Nandal, K. Seki, T. Hisatomi and K. Domen, *Nature*, 2020, **581**, 411-414.

2. M. Wang, Z. Wang, M. Shan, J. Wang, Z. Qiu, J. Song and Z. Li, *Chem. Mater.*, 2023, **35**, 5368-5377.

3. Y. Zhong, W. Dong, S. Ren, L. Li, *Adv. Mater.*, 2024, **36**, 2308251.

4. L. Wang, Q. Xia, M. Hou, C. Yan, Y. Xu, J. Qu and R. Liu, *J. Mater. Chem. B*, 2017, **5**, 9183-9188.

5. Z. Li, Y. Zhi, P. Shao, H. Xia, G. Li, X. Feng, X. Chen, Z. Shi and X. Liu, *Appl. Catal., B*, 2019, **245**, 334-342.

6. G. Wang, S. Li, C. Yan, Q. Li, F. Zhou, Y. Geng and Y. Dong, *Chem. Commun.*, 2020, **56**, 12612-12615.

7. C. Lin, X. Liu, B. Yu, C. Han, L. Gong, C. Wang, Y. Gao, Y. Bian and J. Jiang, *ACS Appl. Mater. Interfaces*, 2021, **13**, 27041-27048.

8. C. Han, X. Sun, X. Liang, L. Wang, H. Hu and X. Liu, *J. Mater. Chem. C*, 2023, **11**, 12000.

9. Z. Zhao, Y. Zheng, C. Wang, S. Zhang, J. Song, Y. Li, S. Ma, P. Cheng, Z. Zhang and Y. Chen, *ACS Catal.*, 2021, **11**, 2098-2107.

10. W. Chen, L. Wang, D. Mo, F. He, Z. Wen, X. Wu, H. Xu and L. Chen, *Angew. Chem. Int. Ed.*, 2020, **59**, 16902-16909.

11. E. Jin, Z. Lan, Q. Jiang, K. Geng, G. Li, X. Wang and D. Jiang, *Chem*, 2019, **5**, 1632-1647.

12. W. Li, X. Huang, T. Zeng, Y. A. Liu, W. Hu, H. Yang, Y. Zhang and K. Wen, *Angew. Chem. Int. Ed.*, 2021, **60**, 1869-1874.